CDF/PHYS/JET/CDFR/10811
Draft 1.2
March 14, 2012

Update of the measurement of the central diphoton production cross section using the full CDF data sample

Ray Culbertson[(1)] and Costas Vellidis[(1)][1]

[(1)] *FNAL*

Abstract

A measurement of the diphoton production cross section at the Tevatron is reported. This is an update of a previous measurement of the same cross section that used CDF Run II data corresponding to 5.4/fb of integrated luminosity. The present measurement is using almost twice as much data, corresponding to 9.5/fb of integrated luminosity, which amounts to the full CDF Run II sample. All techniques concerning background subtraction, acceptance and efficiency determination, calibration and checking are identical to those of the previous measurement. The results are compared with predictions from the parton showering program PYTHIA featuring initial- and final-state radiation at LL accuracy and an underlying event model, the fixed-order NLO program DIPHOX which treats non-perturbative fragmentations at NLO as well, and the NLO program RESBOS which resums initial-state gluon radiation analytically at NNLL accuracy. These calculations were also compared with the results of the previous measurement. In addition to these, three more calculations are compared with the new results: the parton showering program SHERPA, the fixed-order NLO program MCFM, and a recent NNLO calculation.

Contents

[1] vellidis@fnal.gov

1 Introduction

The measurement of the cross section for production of isolated prompt photon pairs in $p\overline{p}$ collisions at the Tevatron allows for testing pQCD calculations and understanding parton interactions at the Tevatron energy of 1.96 TeV. The direct production mechanism, through bremsstrahlung from quarks in the colliding beams, is an irreducible background in the search for a possible Higgs boson in the diphoton decay channel, which is a sensitive channel for a low mass Higgs boson search at the Tevatron and, especially, at the LHC. It is also background to the diphoton decay modes of exotic particles in models beyond the Standard Model. The advance in the understanding of the reaction mechanism which produces this background, through high precision measurements that are now made possible with the high luminosity Tevatron Run II data, allows for a better control of this background and is therefore an important milestone for those searches.

Earlier measurements with CDF Run II data were initially done on a small sample of about 200/pb of integrated luminosity [1], and more recently on a much larger sample of nearly 5.4/fb of integrated luminosity [2], [3], [4], [5]. The main conclusion from the latest measurement was that the theory does not describe well the data in kinematic regions sensitive to non-perturbative fragmentations, corresponding predominantly to diphotons with small invariant mass and large transverse momentum. Furthermore, a parton showering calculation that was found to fail in comparison with the data in the first measurement [1], was now found competitive with more sophisticated NLO calculations if, in addition to the LO direct diphoton production, the prduction of direct photon pairs in LO γ+jet events is properly included as part of NLO corrections, where the second photon in the event comes from initial- or final-state radiation from the colliding quarks.

The present note reports on a third round of the measurement of the cross section for production of central prompt photon pairs using the full CDF Run II data sample that corresponds to 9.5/fb of integrated luminosity. The new results are compared with the calculations compared with the results of the previous measurement, as well as with new calculations complementary to the previous ones. All techniques used in the previous measurement with 5.4/fb of integrated luminosity [2], [3], [4], [5] are applied here unchanged. All details on these techniques are described in the references. This note focuses, therefore, on the checks of the new data, on a brief description of the new calculations compared with the data and on the presentation of the results.

2 Analysis

The data sample used in this analysis is specified by version 45 of the good run list without silicon requirement, recommended for QCD analyses, and corresponds to the full range of data taking periods from 0 through 38, inclusive. The triggers and the offline event selection used are identical with the previous analysis (see [2], [5]) and give a total integrated luminosity of 9.5/fb. The previous analysis used the data taken in the periods from 0 through 25, inclusive. The new data added to the present measurement were taken during the periods from 26 through 38. The analysis factors derived from the data, besides the event yield itself, which can therefore vary with time period, are the correction of the tracking efficiency, the EM energy scale and the cross section for Z→ee, which is measured from "photon-like" selected electrons (see [2], [5]) and is used to cross-check the diphoton cross section measurement. All these factors were checked for their time dependence to ensure that they properly account for the new data.

The MC tracking efficiency correction, derived from the number of vertices distribution in the data, is different for three different ranges of data taking periods: 0-17, 18-25 and 26-38. The 5.4/fb analysis was fully covered by the first two ranges. Adding the data from the third range changes the correction from 0.967 that it was before to 0.969 for 9.5/fb.

The left plot in Fig. 1 shows the EM energy scale variation with the data taking periods. The small variation of about 0.2% observed in the plot is much smaller than the energy scale systematic uncertainty of 1.5% assigned to the measured cross section and can, therefore, be ignored.

The right plot in Fig. 1 shows the variation of the neasured Z→ee cross section with the data taking periods. There is a significant drop of about 10% over the periods 26-38 relative to the average of the periods 0-25 that were used in the previous measurement. The new data in the range of periods 26-38 corresponds to about 42% of the total amount of data used in the full data set analysis. Therefore, the observed drop pulls the measured cross section down by $42\% \times 10\% = 4.2\%$ which is used to correct the diphoton cross section.

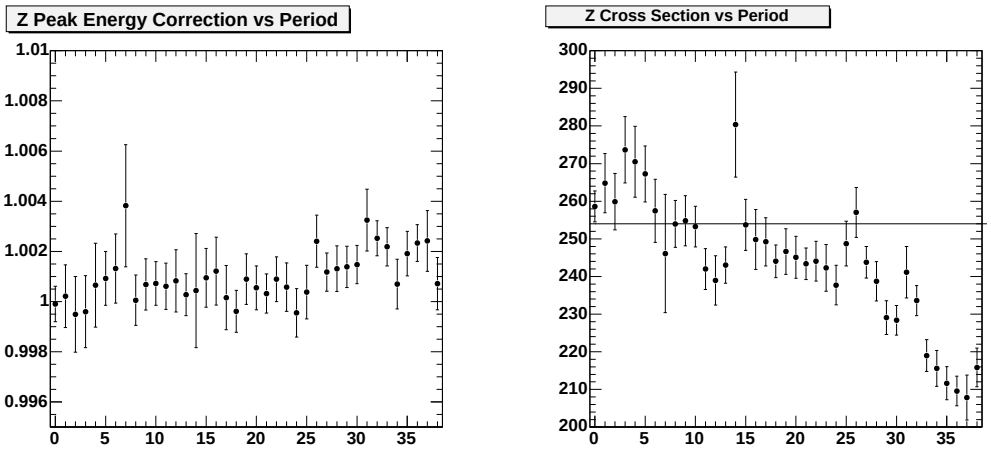

Figure 1: (Left) The EM energy scale as a function of the data taking period. (Right) The measured Z→ee cross section as a function the data taking period.

3 Calculations

The results of this measurement are compared with six theoretical predictions:

1. The parton shower program PYTHIA [6]. The version 6.2.16, built in the standard CDF simulation software, is used. This program is run in a mode where $\gamma\gamma$ and γ+jet events are coherently generated and, from those, only events with (at least) two photons emitted from quarks are filtered. In this way, photons generated either by the PYTHIA $\gamma\gamma$ or γ+jet LO matrix element calculation or by the PYTHIA initial- and final-state radiation model are taken into account, simulating in part (real) NLO corrections to the basic $\gamma\gamma$ LO matrix element calculation. The proton PDF set used in this calculation is CTEQ5L [7].

2. The fixed-order NLO program DIPHOX [8] which includes explicit non-perturbative fragmentations [9] treated at NLO. The version 1.2 of the program is used. The proton PDF set used in this calculation is CTEQ6.1M [7] and the renormalization, factorization and fragmentation scales are all set to the event's $\gamma\gamma$ invariant mass.

3. The program RESBOS [10] which resums the initial-state gluon radiation analytically at NNLL accuracy at low diphoton transverse momentum and then it smoothly matches this "soft" contribution with the "hard" contribution from the NLO matrix element, valid at high diphoton transverse momentum. The proton PDF set used in this calculation is CTEQ6.6M [7] and the renormalization and factorization scales are all set to half the event's $\gamma\gamma$ invariant mass.

4. The fixed-order NLO program MCFM [11] which includes explicit non-perturbative fragmentations [12] treated at LO. The proton PDF set used in this calculation is MSTW8NL [7] and the renormalization, factorization and fragmentation scales are all set to the event's $\gamma\gamma$ invariant mass.

5. The parton shower program SHERPA [13]. The version 1.3.1 of this program is used. The proton PDF set used in this calculation is CTEQ6.6M [7]. This program features NLO aspects and a smoother transition from "hard" (perturbative) to "soft" (non-perturbative) physics compared with PYTHIA.

6. A recent "q_T"-subtracted NNLO calculation [14], compared with Tevatron data for the first time here.

The PYTHIA, DIPHOX and RESBOS calculations are the same that were used in the 5.4/fb measurement and they are extensively discussed in references [2] and [5]. MCFM is similar to DIPHOX but with a different definition and treatment of the non-perturbative fragmentations.

The kinematic and photon isolation cuts applied to the data at the hadron (observable particle) level are also applied to the calculations. For the NLO calculations,

which provide only parton-level predictions, the isolation cut involves some approximation. Theoretical uncertainties are currently estimated only for the NLO calculations, where they are more unambiguously defined. They amount to the scale and PDF uncertainties, added in quadrature. The scale uncertainties are stimated by varying the scales simultaneously up and simultaneously down by a factor of two relative to the default choices. The PDF uncertanites are estimated by varying the eigenvectors of the selected PDF set within their uncertainties [7].

	Cross section (pb)
Data from 5.4 fb^{-1}	$12.47 \pm 0.21_{\text{stat}} \pm 3.74_{\text{syst}}$
Data from 9.5 fb^{-1}	$12.32 \pm 0.15_{\text{stat}} \pm 3.39_{\text{syst}}$
RESBOS	$11.31 \pm 2.45_{\text{syst}}$
DIPHOX	$10.58 \pm 0.55_{\text{syst}}$
PYTHIA $\gamma\gamma + \gamma$j	9.19
MCFM	11.63
SHERPA	8.29

Table 1: The total diphoton production cross section obtained from the measurement and from the theoretical calculations.

4 Results

The total cross sections are shown in Table 1. The results for the differential cross sections are presented in plots as functions of various kinematic variables, which are defined in references[2] and [5], and for three different kinematic conditions: unconstrained; diphoton transverse momentum larger than diphoton mass; and diphoton transverse momentum smaller than diphoton mass. The meaning of each condition is extensively discussed in these references. The comparison with the theoretical predictions is currently being worked. The NNLO calculations are not yet added. PYTHIA is shown again instead, as a place holder until the calculations are sent by the authors. Sample plots of the cross section results for unconstrained kinematics are shown here. The plots with the new calculations are not commented because these calculations are not yet final. For the old calculations, the comments given in [5] apply. All plots can be found in reference [15]. For each kinematic variable the following set os plots is provided:

- The convoluted acceptance×efficiency providing the normalization of the cross section in each bin.
- The systematic uncertainties in each bin, shown as histograms for the corresponding kinematic variable.
- The measured differential cross section compared with three calculations.
- The relative deviation of the measured cross section from each prediction, presented in the form (data - theory)/theory.

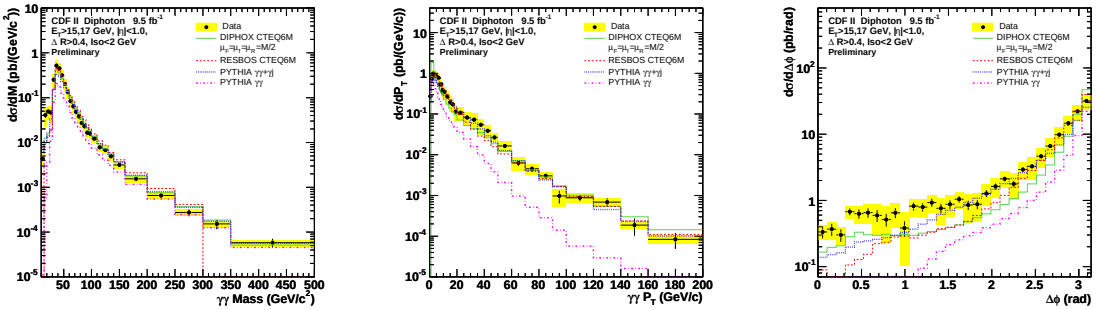

Figure 2: (Left) Cross sections differential in the diphoton mass. (Middle) Cross sections differential in the diphoton transverse momentum. (Right) Cross sections differential in the diphoton azimuthal difference.

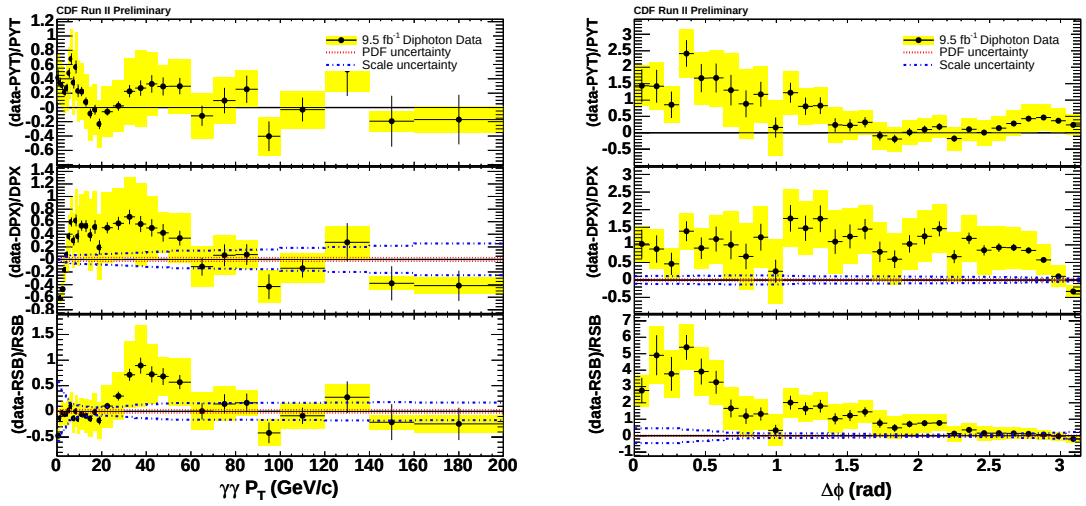

Figure 3: (Left) Data-to-theory ratios differential in the diphoton transverse momentum. (Right) Data-to-theory ratios differential in the diphoton azimuthal difference.

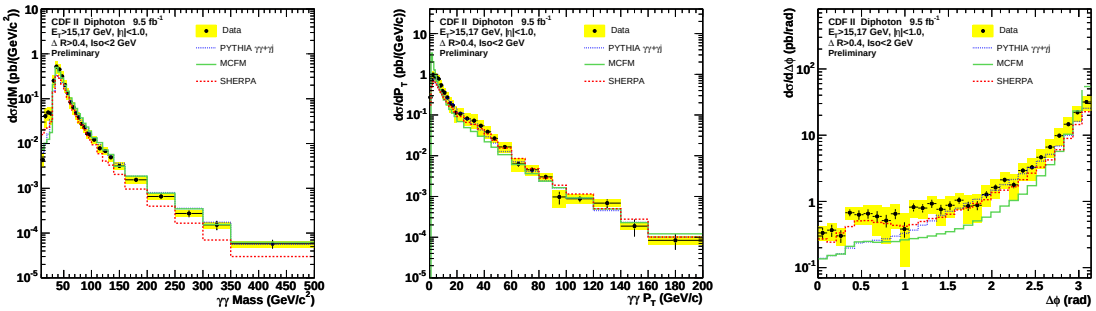

Figure 4: (Left) Cross sections differential in the diphoton mass. (Middle) Cross sections differential in the diphoton transverse momentum. (Right) Cross sections differential in the diphoton azimuthal difference.

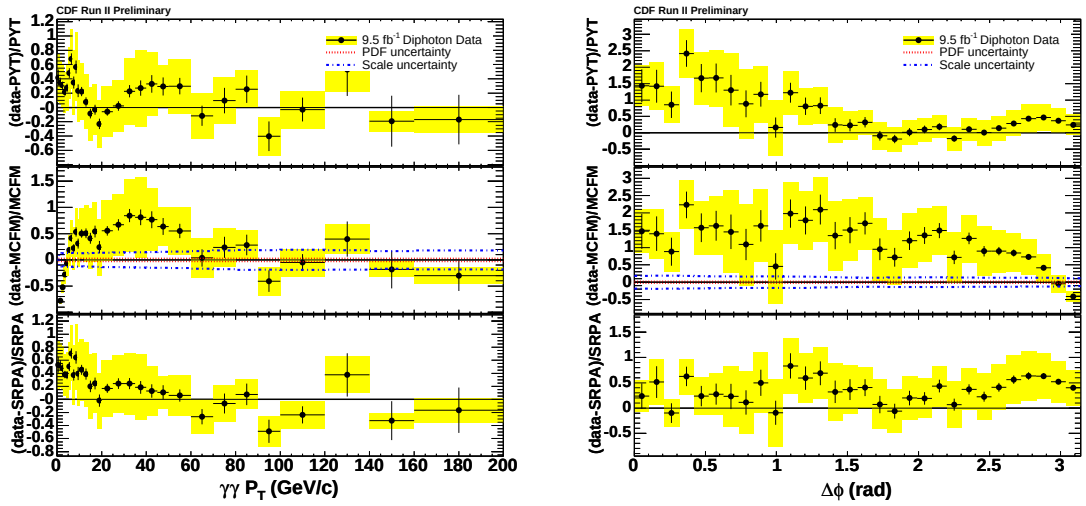

Figure 5: (Left) Data-to-theory ratios differential in the diphoton transverse momentum. (Right) Data-to-theory ratios differential in the diphoton azimuthal difference.

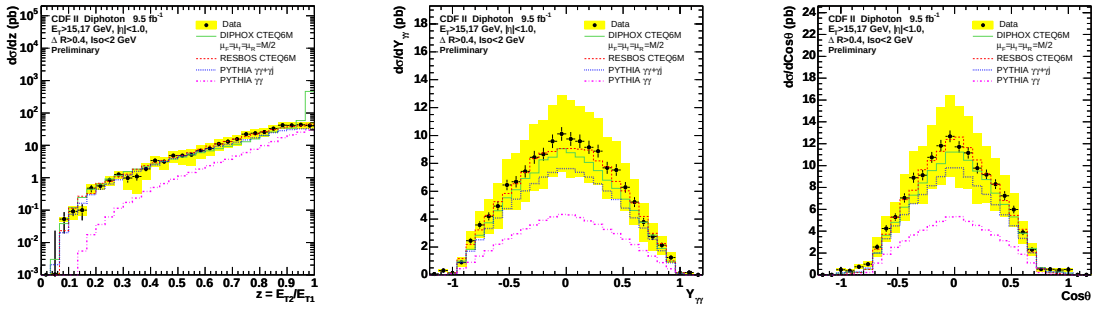

Figure 6: (Left) Cross sections differential in the photon transverse momentum ratio. (Middle) Cross sections differential in the diphoton rapidity. (Right) Cross sections differential in the cosine of the diphoton Collins-Soper polar angle.

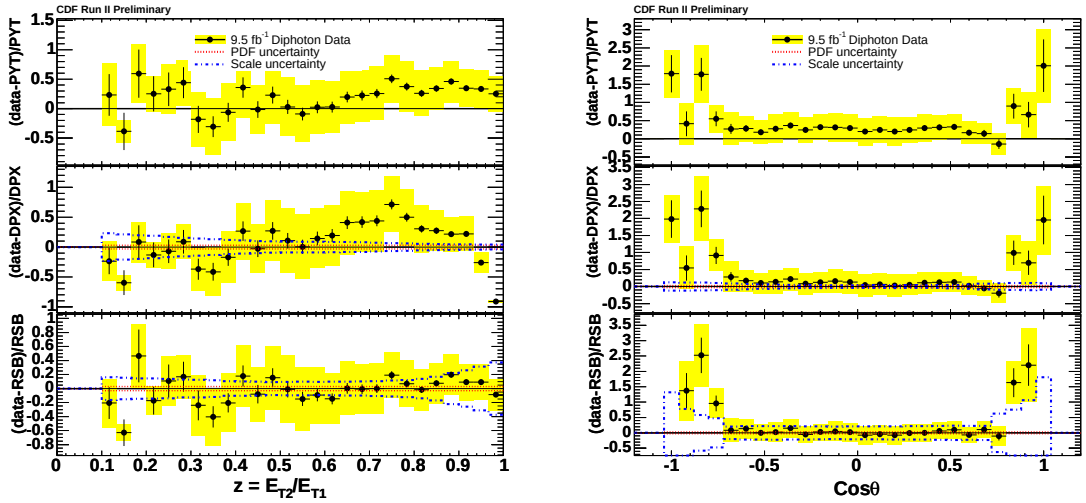

Figure 7: (Left) Data-to-theory ratios differential in the photon transverse momentum ratio. (Right) Data-to-theory ratios differential in the cosine of the diphoton Collins-Soper polar angle.

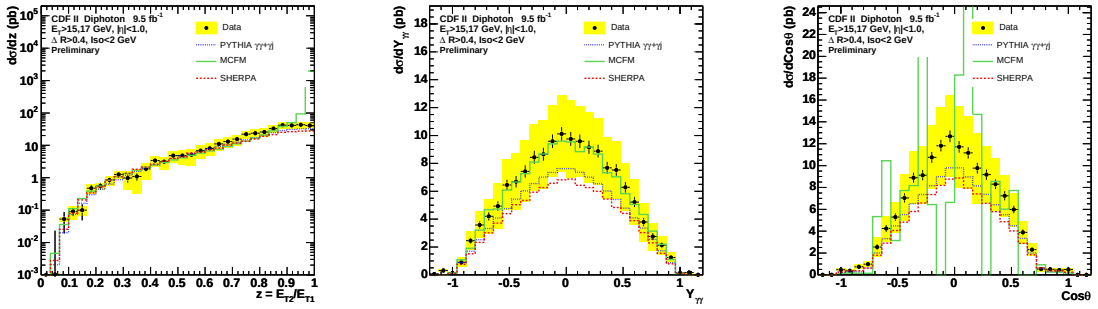

Figure 8: (Left) Cross sections differential in the photon transverse momentum ratio. (Middle) Cross sections differential in the diphoton rapidity. (Right) Cross sections differential in the cosine of the diphoton Collins-Soper polar angle.

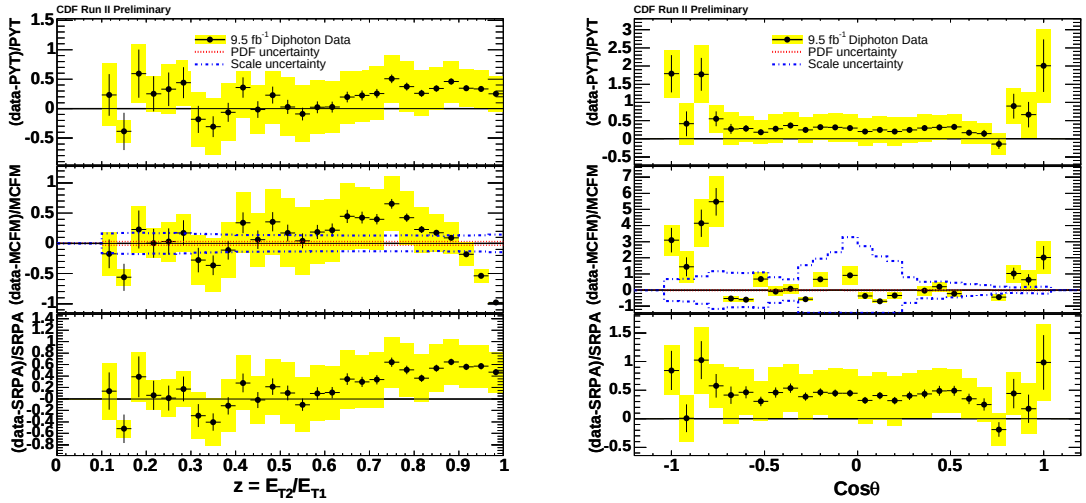

Figure 9: (Left) Data-to-theory ratios differential in the photon transverse momentum ratio. (Right) Data-to-theory ratios differential in the cosine of the diphoton Collins-Soper polar angle.

5 Conclusions

The central prompt diphoton cross section, previously measured with CDF Run II data of 5.4/fb integrated luminosity, is now measured with data of 9.5/fb integrated luminosity, corresponding to the full CDF Run II data sample. The updated measurement retains all techniques from the previous measurement and consistent results are found. The measured distributions are compared with predictions from six different theoretical calculations, complementary in their assumptions and methods. Partial agreement between data and theory is found. This is the most complete measurement of diphoton differential cross sections at the Tevatron.

References

[1] R. Culbertson *et al*, "Isolated prompt diphoton central-central cross section measurement at CDF Run II", CDFNote 6312, August 2004.

[2] R. Culbertson *et al*, "Measurement of the central diphoton production cross section at CDF", CDFNote 10009, April 2010.

[3] R. Culbertson *et al*, "Measurement of the Cross Section for Prompt Diphoton Production with 5.4/fb of CDF Run II Data", CDFNote 10160, May 2010.

[4] T. Aaltonen *et al.* (CDF Collaboration), "Measurement of the Cross Section for Prompt Isolated Diphoton Production in $p\bar{p}$ Collisions at $\sqrt{s}$=1.96 TeV", Phys. Rev. Lett. **107**, 102003 (2011); arXiv: 1106.5123.

[5] T. Aaltonen *et al.* (CDF Collaboration), "Measurement of the Cross Section for Prompt Isolated Diphoton Production in $p\bar{p}$ Collisions at $\sqrt{s}$=1.96 TeV", Phys. Rev. D **84**, 052006 (2011). arXiv: 1106.5131.

[6] T. Sjöstrand *et al.*, Comp. Phys. Comm. **135**, 238 (2001).

[7] J. Pumplin *et al*, "New Generation of Parton Distributions with Uncertainties from Global QCD Analysis", arXiv:hep-ph/0201195, February 2002.

[8] T. Binoth *et al*, "A full Next to Leading Order study of direct photon pair production in hadronic collisions", arXiv:hep-ph/9911340v3, April 2000.

[9] L. Bouhris *et al.*, Eur. Phys. J. **C2**, 529 (1998).

[10] T. Balazs *et al*, "Calculation of prompt diphoton production cross sections at Tevatron and LHC energies", arXiv:hep-ph/9911340v3, April 2000.

[11] J. M. Campbell *et al.*, Phys. Rev. D **60**, 113006 (1999).

[12] A. Gehrmann-De Ridder *et al.*, Eur. Phys. J. C **7**, 29 (1999).

[13] T. Gleisberg *et al.*, JHEP **02**, 007 (2009).

[14] L. Cieri *et al.*, arXiv: 1110.2375 (2011).

[15] http://www-cdf.fnal.gov/∼vellidis/internal/diphoton/plots/07Mar12/